Proton-neutron coupling in the Gamow shell model: The lithium chain

N. Michel,[1,2,3,*] W. Nazarewicz,[1,2,4,†] and M. Płoszajczak[5,‡]

[1]*Department of Physics and Astronomy, University of Tennessee, Knoxville, Tennessee 37996, USA*
[2]*Physics Division, Oak Ridge National Laboratory, P. O. Box 2008, Oak Ridge, Tennessee 37831, USA*
[3]*Joint Institute for Heavy-Ion Research, Oak Ridge, Tennessee 37831, USA*
[4]*Institute of Theoretical Physics, Warsaw University, ulica Hoża 69, 00-681 Warsaw, Poland*
[5]*Grand Accélérateur National d'Ions Lourds (GANIL), CEA/DSM-CNRS/IN2P3, Boîte Postale 55027,*
F-14076 Caen Cedex 05, France

The shell model in the complex-k plane (the so-called Gamow shell model) has recently been formulated and applied to the structure of weakly bound, neutron-rich nuclei. The completeness relations of Newton and Berggren, which apply to the neutron case, are strictly valid for finite-range potentials. However, for long-range potentials, such as the Coulomb potential for protons, for which the arguments based on the Mittag-Leffler theory do not hold, the completeness still needs to be demonstrated. This has been done in this paper, both analytically and numerically. The generalized Berggren relations are then used in the first Gamow shell model study of nuclei having *both* valence neutrons and protons, namely, the lithium chain. The single-particle basis used is that of the Hartree-Fock-inspired potential generated by a finite-range residual interaction. The effect of isospin mixing in excited unbound states is discussed.

I. INTRODUCTION

One of the main frontiers of the nuclear many-body problem is the structure of exotic, short-lived nuclei with extreme neutron-to-proton ratios. Apart from intrinsic nuclear structure interest, properties of these nuclei are crucial for our understanding of astrophysical processes responsible for cooking of elements in stars. From a theoretical point of view, the major challenge is to achieve a consistent picture of structure and reaction aspects of weakly bound and unbound nuclei, which requires an accurate description of the particle continuum [1]. Here, the tool of choice is the continuum shell model (see Ref. [2] for a recent review) and, most recently, the Gamow shell model (GSM) [3–6] (see also Refs. [7–9]). The GSM is the multiconfigurational shell model with a single-particle (s.p.) basis given by the Berggren ensemble [10–12] which consists of Gamow (or resonant) states and the complex nonresonant continuum. The resonant states are the generalized eigenstates of the time-independent Schrödinger equation which are regular at the origin and satisfy purely outgoing boundary conditions. The s.p. Berggren basis is generated by a finite-depth potential, and the many-body states are obtained in shell-model calculations as the linear combination of Slater determinants spanned by resonant and nonresonant s.p. basis states. Hence, both continuum effects and correlations between nucleons are taken into account simultaneously. The interested reader can find all details of the formalism in Ref. [4], in which the GSM was applied to many-neutron configurations in neutron-rich helium and oxygen isotopes.

When extending the GSM formalism to the general neutron-proton case, with both protons and neutrons occupying valence s.p. states, one is confronted with a theoretical problem: the Berggren completeness relations, which are the pillars of the Gamow shell model, have been strictly proved (and checked numerically [4,13]) only for quickly vanishing (finite-range) local potentials, while the repulsive Coulomb potential for protons has infinite range. The theoretical problem lies, in fact, not in the Berggren (complex-energy) completeness relation itself, but in the Newton (real-energy) completeness relation [14,15]. This latter involves both bound and scattering states, upon which the Berggren completeness relations can be demonstrated using the method of analytic continuation.

Our paper is organized as follows. Section II contains a derivation of the Newton completeness relation that is valid for a rather wide class of potentials, including the Coulomb potential. Based on this result, the Berggren completeness relation for protons is derived in the same way as previously done for neutrons [4]. The numerical tests of the completeness of the proton Berggren ensemble are given in Sec. III. Section IV introduces the Hartree-Fock- (HF-)inspired procedure used to optimize the s.p. basis, the so-called Gamow-HF method. The first GSM calculation involving active neutrons and protons is presented in Sec. V, with the 1p-shell study of the lithium chain, ranging from ^{5}Li to ^{11}Li. The residual interaction used is a surface-peaked finite range force. A novel aspect, absent in our previous GSM studies, is the appearance of $T=0$ couplings which seem to exhibit significant particle-number (or density) dependence. Finally, Sec. VI contains the main conclusions of our work.

II. COMPLETENESS RELATIONS IN THE GSM: ANALYTICAL CONSIDERATIONS

As the one-body completeness relation for resonant and scattering states is prerequisite for our theory, we shall dem-

---

*Electronic address: michel@mail.phy.ornl.gov
†Electronic address: witek@utk.edu
‡Electronic address: ploszajczak@ganil.fr

onstrate it rigorously. We shall first consider the case of a local potential and then generalize it to nonlocal potentials.

A. Local potential

In order to demonstrate the orthonormality and completeness relations for s.p. proton states, we consider a spherical proton potential that is finite at $r=0$, and it has a pure Coulomb behavior for $r \to +\infty$. The one-body radial wave functions $u(r)$ are solutions of the Schrödinger equation:

$$u''(r) = \left[\frac{l(l+1)}{r^2} + v(r) - k^2 \right] u(r), \qquad (1)$$

$$v(r) \sim \frac{\text{const}}{r}, \quad r \to +\infty, \qquad (2)$$

where the potential v is given in units of fm^{-2}, and l is the angular momentum of the particle. Let us consider the bounded region enclosed in a large sphere of radius R. (This can be achieved by introducing an infinite well of radius R surrounding the nucleus.) Of course, in the final result, R will be allowed to go to infinity. For each value of R, one has the following completeness relation on $[0:R]$ [16]:

$$\sum_{n \in b} u_n(r) u_n(r') + \sum_{m=0}^{+\infty} u^{(d)}(k_m, r) u^{(d)}(k_m, r') = \delta(r - r'), \qquad (3)$$

where b denotes the set of bound states having radial wave functions $u_n(r)$ with $k_n^2 < v(R)$, and $u^{(d)}(k_m, r)$ is a wave function of a normalized discretized continuum state, given by the boundary conditions $u^{(d)}(k_m, 0) = 0$ and $u^{(d)}(k_m, R) = 0$.

For the purpose of this discussion, it is convenient to introduce the set of wave functions [12]

$$u(k_i, r) = \frac{u^{(d)}(k_i, r)}{\sqrt{k_{i+1} - k_i}}, \qquad (4)$$

which obey the following normalization condition:

$$\langle u(k_i) | u(k_j) \rangle = \frac{\delta_{ij}}{k_{i+1} - k_i}. \qquad (5)$$

Since, in addition,

$$\langle u(k) | u_n \rangle = 0, \qquad (6)$$

$$\langle u_n | u_{n'} \rangle = \delta_{nn'}, \qquad (7)$$

the box completeness relation can be written as

$$\sum_{n \in b} u_n(r) u_n(r') + \sum_{m=0}^{+\infty} u(k_m, r) u(k_m, r')(k_{m+1} - k_m) = \delta(r - r'). \qquad (8)$$

When $R \to +\infty$, the infinite series in Eq. (8) becomes an integral, thus giving the expected completeness relation. Unfortunately, this cannot be done right away, as the series and the integral converge only in a weak sense.

To prove the convergence rigorously, let us consider the completeness relation of the free box expressed in the form of Eq. (4):

$$\sum_{m=0}^{+\infty} B_m^2 \hat{j}_l(\kappa_m r) \hat{j}_l(\kappa_m r')(\kappa_{m+1} - \kappa_m) = \delta(r - r'), \qquad (9)$$

where $\hat{j}_l(\kappa_m r')$ are the Riccati-Bessel functions, $\hat{j}_l(\kappa_m R) = 0$ ($m = 0, 1, 2 \ldots$), and B_m is the normalization constant

$$-B_m^2 \frac{R}{2} \hat{j}_{l+1}(\kappa_m R) \hat{j}_{l-1}(\kappa_m R) = \frac{1}{\kappa_{m+1} - \kappa_m}. \qquad (10)$$

Subtracting (9) from (8), one obtains

$$\sum_{n \in b} u_n(r) u_n(r') + \sum_{m=0}^{+\infty} [u(k_m, r) u(k_m, r')(k_{m+1} - k_m)$$
$$- B_m^2 \hat{j}_l(\kappa_m r) \hat{j}_l(\kappa_m r')(\kappa_{m+1} - \kappa_m)] = 0. \qquad (11)$$

We shall now demonstrate that the above series converges in the sense of functions, so the limiting transition from a series to an integral when $R \to +\infty$ can be easily carried out.

To this end, let us consider the behavior of the mth term in the series when m (and $k_m) \to +\infty$. For very large values of k_m, one can use the semiclassical expansion in powers of k_m^{-1}:

$$u(k_m, r) = C_m \hat{j}_l(k_m r) - C_m \frac{\mathcal{V}(r)}{2k_m} \hat{j}_l'(k_m r) + O\left(\frac{C_m}{k_m^2} \right), \quad (12)$$

$$\hat{j}_l(k_m r) = \sin\left(k_m r - l\frac{\pi}{2} \right) - \frac{a_l}{2k_m r} \cos\left(k_m r - l\frac{\pi}{2} \right) + O\left(\frac{1}{k_m^2 r^2} \right), \qquad (13)$$

where C_m is a normalization constant, a_l is a constant depending on l only, and

$$\mathcal{V}(r) = \int_0^r v(r') dr'. \qquad (14)$$

For the Coulomb potential, $\mathcal{V}(r) \propto \ln r$; hence the expression (12) properly accounts for the logarithmic term in the phase shift. It immediately follows from Eqs. (12) and (13) that

$$k_m = \frac{(m + 1/2)\pi}{R} + \frac{a_l + R\mathcal{V}(R)}{2Rm\pi} + O\left(\frac{1}{m^2} \right), \qquad (15)$$

$$\kappa_m = \frac{(m + 1/2)\pi}{R} + \frac{a_l}{2Rm\pi} + O\left(\frac{1}{m^2} \right). \qquad (16)$$

The constant C_m can be determined from the normalization condition:

$$C_m^2 \int_0^R \left[\hat{j}_l^2(k_m r) - \frac{\mathcal{V}(r)}{k_m} \hat{j}_l(k_m r) \hat{j}_l'(k_m r) \right] dr + O\left(\frac{C_m^2}{k_m^2} \right)$$
$$= \frac{1}{k_{m+1} - k_m}. \qquad (17)$$

Since the integral involving $\mathcal{V}$ behaves like $1/k_m^2$, C_m becomes

$$C_m^2 \frac{R}{2}\left[\hat{j}_l^2(k_m R) - \hat{j}_{l+1}(k_m R)\hat{j}_{l-1}(k_m R)\right] + O\left(\frac{C_m^2}{k_m^2}\right) = \frac{1}{k_{m+1} - k_m} \tag{18}$$

[cf. Eq. (10)].

Using Eqs. (15) and (16), one obtains

$$C_m = \sqrt{\frac{2}{\pi}} + O\left(\frac{1}{m^2}\right), \tag{19}$$

$$B_m = \sqrt{\frac{2}{\pi}} + O\left(\frac{1}{m^2}\right). \tag{20}$$

Let us consider the behavior of B_m for $R \to +\infty$ but $\kappa_m \to \kappa$ with $\kappa > 0$. The expansion of Eq. (13) is still valid in this case, as for $r = R$, it is a familiar expansion in $1/R$ of the Bessel function. It follows from Eq. (13) that

$$\kappa_m = \frac{(m + 1/2)\pi}{R} + O\left(\frac{1}{R^2}\right) \tag{21}$$

with m chosen so κ_m is the closest to κ. Then Eqs. (10) and (13) give

$$B_m = \sqrt{\frac{2}{\pi}} + O\left(\frac{1}{R}\right), \tag{22}$$

as expected.

Note that the leading term in Eqs. (19) and (20) is the familiar normalization of continuum wave functions [17]. The reminders, of the order of m^{-2}, guarantee the convergence of the series. By using Eqs. (12)–(16), one can show that the series (11) converges for all $r > 0$ and $r' > 0$.

As a consequence, in the limit of $R \to +\infty$, Eq. (11) becomes

$$\sum_{n \in b} u_n(r)u_n(r') + \int_0^{+\infty}\left[u(k,r)u(k,r') - \frac{2}{\pi}\hat{j}_l(kr)\hat{j}_l(kr')\right]dk$$
$$= 0. \tag{23}$$

By taking advantage of the closure relation for the Riccati-Bessel functions,

$$\int_0^{+\infty}\hat{j}_l(kr)\hat{j}_l(kr')dk = \frac{\pi}{2}\delta(r - r'), \tag{24}$$

one finally arrives at the sought completeness relation

$$\sum_{n \in b} u_n(r)u_n(r') + \int_0^\infty u(k,r)u(k,r')dk = \delta(r - r'). \tag{25}$$

By using the same arguments as in Ref. [4], one obtains the generalized Berggren completeness relation, also valid for the proton case:

$$\sum_{n \in b,d} u_n(r)u_n(r') + \int_{L^+} u(k,r)u(k,r')dk = \delta(r - r'). \tag{26}$$

For details, including the numerical treatment of scattering wave functions and corresponding matrix elements, we refer the reader to Ref. [4]. Let us only remark, in passing, that in the presence of the Coulomb potential the standard regularization procedure [18,19] has to be modified [20]. In our work, however, we apply the exterior complex scaling method [21,22] which works very well regardless of whether the Coulomb potential is used or not.

B. Nonlocal potential

In the presence of a nonlocal potential, such as the HF exchange potential generated by a finite-range two-body interaction, the Schrödinger equation (1) becomes

$$u''(r) = \left[\frac{l(l + 1)}{r^2} + v_l(r) - k^2\right]u(r) + \int_0^{+\infty}v_{nl}(r,r')u(r')dr' \tag{27}$$

where v_l is the local part of the potential, and v_{nl} its nonlocal kernel. We assume that $v_{nl}(r,r') \to 0$ when $r \to +\infty$ or $r' \to +\infty$ (the nuclear potential has to be localized) and that $v_{nl}(r,0) = 0 \forall r$ (the potential is regular at the origin). As the radial HF functions are regular at zero, the latter condition is automatically met for the HF exchange potential.

If the integral containing the nonlocal potential v_{nl} behaves like $1/k^2$ when $k \to +\infty$, then the asymptotic expression (12) holds. Indeed, integration by parts yields

$$\int_0^{+\infty}v_{nl}(r,r')\left[j_l(kr') - \frac{\mathcal{V}_l(r')j_l'(kr')}{2k}\right]dr'$$
$$= \frac{1}{k^2}\left[\frac{\partial v_{nl}}{\partial r'}(r,0)\mathcal{J}_l(0) + \int_0^{+\infty}\frac{\partial^2 v_{nl}}{\partial r'^2}(r,r')\mathcal{J}_l(kr')dr'\right]$$
$$+ O\left(\frac{1}{k^2}\right) = O\left(\frac{1}{k^2}\right), \tag{28}$$

where $\mathcal{V}_l(r) = \int_0^r v_l(r')dr'$, $\mathcal{J}_l(t) = \int_{t_0}^t \int_{t_0'}^{t'} j_l(t'')dt''dt'$, and t_0 and t_0' are chosen so that $\mathcal{J}_l(t)$ is bounded on $[0 : +\infty[$. Consequently, Eq. (12) also holds for nonlocal potentials. The proof of completeness can be, therefore, performed in the same way as for local potentials, by simply replacing v by v_l in all expansions in k^{-1}.

III. COMPLETENESS OF THE ONE-BODY PROTON BERGGREN ENSEMBLE: NUMERICAL TESTS

In this section, we shall discuss examples of the Berggren completeness relation in the one-proton case (for the neutron case, see Ref. [4]). The s.p. basis is generated by the spherical Woods-Saxon (WS) plus Coulomb potential:

$$V(r) = -V_0 f(r) - 4V_{so}\mathbf{l}\cdot\mathbf{s}\frac{1}{r}\frac{df(r)}{dr} + V_c(r), \tag{29}$$

$$f(r) = \left[1 + \exp\left(\frac{r - R_0}{d}\right)\right]^{-1}. \tag{30}$$

In all the examples of this section, the WS potential has the radius $R_0 = 5.3$ fm, the diffuseness $d = 0.65$ fm, and the spin-orbit strength $V_{so} = 5$ MeV. The Coulomb potential V_c is as-
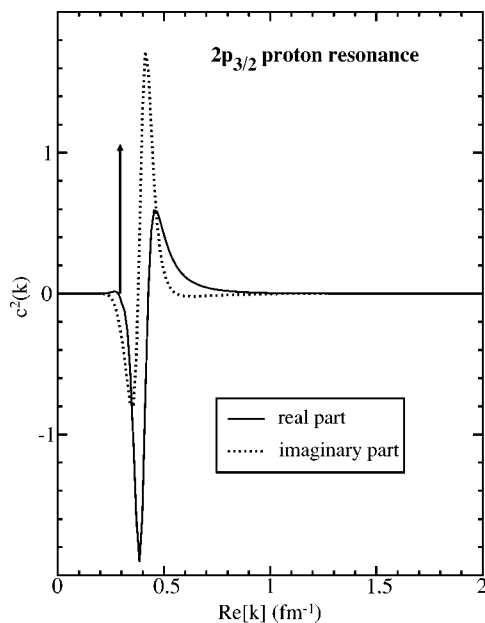
FIG. 1. Distribution of the squared amplitudes $c^2(k)$ of the $2p_{3/2}$ proton state of a Woods-Saxon potential with a depth $V_0 = 65$ MeV, in the s.p. basis generated by a Woods-Saxon potential with a depth $V_0 = 70$ MeV. The Coulomb potential is assumed to be that of a uniformly charged sphere. The amplitudes of both real (solid line) and imaginary (dotted line) components of the wave function are plotted as a function of Re[k]. The height of the arrow gives the squared amplitude of the $2p_{3/2}$ state contained in the basis.

sumed to be generated by a uniformly charged sphere of radius R_0 and charge $Q = +20e$. The depth of the central part is varied to simulate different situations.

In this section, we shall expand the $2p_{3/2}$ state $|u_{\text{WS}}\rangle$, either weakly bound or resonant, in the basis $|u_{\text{WS}^B}(k)\rangle$ generated by the WS potential of a different depth:

$$|u_{\text{WS}}\rangle = \sum_i c_{k_i} |u_{\text{WS}^B}(k_i)\rangle + \int_{L_+} c(k) |u_{\text{WS}^B}(k)\rangle dk \quad (31)$$

[cf. Eq. (26)]. In the above equation, the first term in the expansion represents contributions from the resonant states while the second term is the nonresonant continuum contribution. Since the basis is properly normalized, the expansion amplitudes meet the condition

$$\sum_i c_{k_i}^2 + \int_{L_+} c^2(k) dk = 1. \quad (32)$$

In all cases considered, the $0p_{3/2}$ and $1p_{3/2}$ orbitals are well bound (by ~ 50 and ~ 20 MeV, respectively) and do not play any significant role in the expansion studied, although they are taken into account in the actual calculation. The $2p_{3/2}$ state is, however, either loosely bound or resonant, and the scattering states along the contour L_+ are essential to guarantee the completeness. To take the nonresonant continuum into account, we take the complex contour L_+ that corresponds to three straight segments in the complex-k plane, joining the points $k_0 = 0.0 - i0.0$, $k_1 = 0.3 - i0.1$, $k_2 = 1.0 - i0.0$,
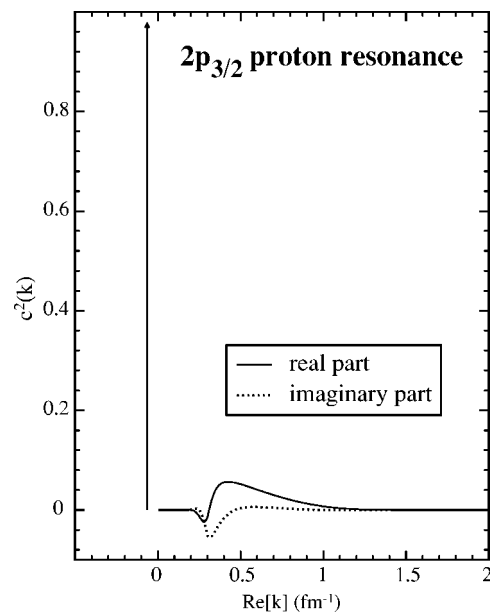

FIG. 2. Similar to Fig. 1 except for the bound $2p_{3/2}$ s.p. state of the WS potential with $V_0 = 75$ MeV expanded in the basis generated by another WS potential ($V_0^{(B)} = 80$ MeV). The height of the arrow gives the squared amplitude of the bound $2p_{3/2}$ state at the value of $-\text{Im}[k]$. (The corresponding k value is purely imaginary.)

and $k_3 = 2.0 - i0.0$ (all in fm^{-1}). The contour is discretized with $n = 40$ points:

$$|2p_{3/2}\rangle \simeq \sum_{n \in b,d} c_n |u_n\rangle + \sum_{i=1}^n c_{k_i} |u(k_i)\rangle. \quad (33)$$

In the first example, we shall expand the $2p_{3/2}$ s.p. resonance ($E = 3.287$ MeV, $\Gamma = 931$ keV) of a WS potential of the depth $V_0 = 65$ MeV in the basis generated by the WS potential of the depth $V_0^B = 70$ MeV. (Here the $2p_{3/2}$ s.p. resonance has an energy $E = 1.905$ MeV and width $\Gamma = 61.89$ keV.) After diagonalization in the discretized basis (33), one obtains $E = 3.289$ MeV and $\Gamma = 934$ keV for the $2p_{3/2}$ s.p. resonance, i.e., the discretization error is ~ 3 keV. The density of the expansion amplitudes is shown in Fig. 1. As both states are resonant, the squared amplitude of the $2p_{3/2}$ basis state is close to 1. Nevertheless, the contribution from the nonresonant continuum is essential. It is due to the fact that the resonant state in the basis is very narrow, whereas the expanded resonant state is fairly broad. It is interesting to notice that the contribution from scattering states with energies smaller than that of the resonant state is practically negligible; this is due to the confining effect of the Coulomb barrier.

The second example, shown in Fig. 2, deals with the case of a $2p_{3/2}$ state that is bound in both potentials. Here $V_0 = 75$ MeV and $V_0^{(B)} = 80$ MeV, and the $2p_{3/2}$ state lies at $E = -0.0923$ MeV and $E = -2.569$ MeV, respectively. Here, the scattering component is almost negligible, which reflects the localized character of bound proton states. After the diagonalization, one obtains $E = -2.568$ MeV and $\Gamma = 1.73$ keV for the $2p_{3/2}$ state, which is indeed very close to the exact result.
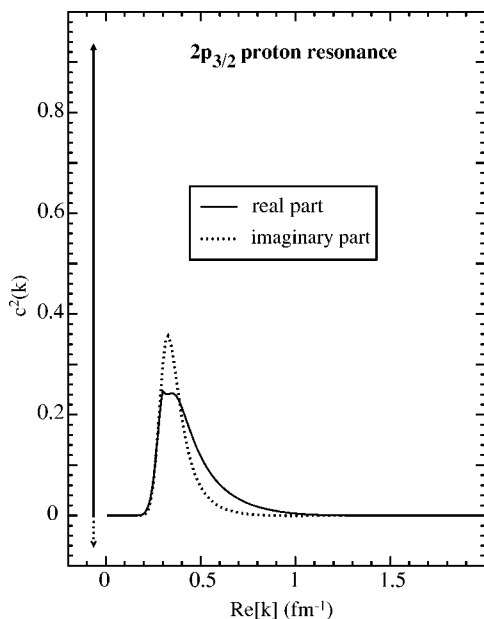
FIG. 3. Similar to Fig. 2 except for the $2p_{3/2}$ resonance of the WS potential with $V_0 = 70$ MeV expanded in the basis generated by another WS potential ($V_0^{(B)} = 75$ MeV).
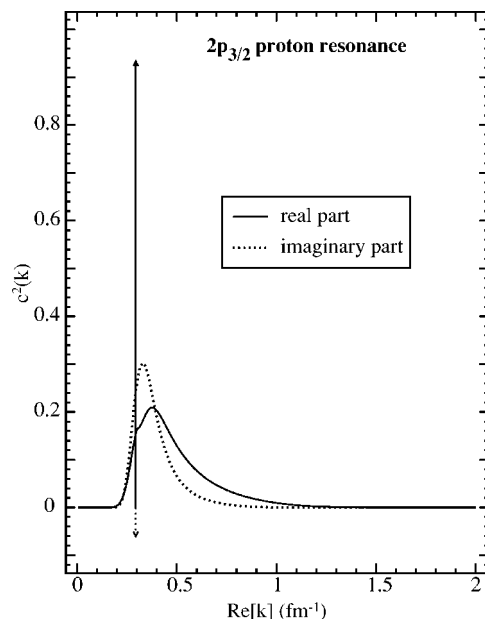

FIG. 4. Similar to Fig. 2 except for the $2p_{3/2}$ resonance of the WS potential with $V_0 = 75$ MeV expanded in the basis generated by another WS potential ($V_0^{(B)} = 70$ MeV).

In the third example (Fig. 3), the unbound $2p_{3/2}$ state ($E = 1.905$ MeV and $\Gamma = 61.89$ keV; $V_0 = 70$ MeV) is expanded in a WS basis containing the bound $2p_{3/2}$ level ($E = -0.0923$ MeV; $V_0^{(B)} = 75$ MeV). As a consequence, the resonance's width has to be brought by the scattering states. Nevertheless, the component of the $2p_{3/2}$ state of the basis is still close to 1, whereas the continuum component plays a secondary role. Once again, one can see a Coulomb barrier effect: even if the expanded $2p_{3/2}$ state is unbound, its wave function is very localized due to the large Coulomb barrier; hence it has a large overlap with the bound $2p_{3/2}$ basis state. The diagonalization yields $E = 1.9065$ MeV and $\Gamma = 58.9$ keV, i.e., the discretization error is again close to 3 keV.

In the last example, shown in Fig. 4, the basis is that of the WS potential with a depth of 70 MeV, and the expanded state corresponds to a WS potential with $V_0 = 75$ MeV. This is the most interesting case since one expresses a bound (real) state in a basis that contains only complex wave functions. (The contribution from well bound $0p_{3/2}$ and $1p_{3/2}$ s.p. states is negligible.) As expected, the behavior of the amplitudes is very close to that of the previous example (see Fig. 3). Moreover, one can notice that the scattering states become important in the expansion when their energies approach the resonant state energy. The diagonalization gives $E = -0.0925$ MeV and $\Gamma = -3.8$ keV for the $2p_{3/2}$ state.

Summarizing this section, our numerical tests demonstrate that the one-body Berggren completeness relation works very well in the proton case involving the Coulomb potential. For other numerical tests, see Refs. [23] (study of the s.p. level density) and [24] (study of the Berggren expansion in the pole approximation).

IV. SPHERICAL GAMOW HARTREE-FOCK METHOD

In our previous calculations of the He chain [3,4], we used the s.p. basis of the WS potential representing ^{5}He. This

basis is appropriate at the beginning of the He chain, but when departing from the core nucleus, its quality deteriorates. For instance, the "^{5}He" basis is not expected to be optimal when applied to the neutron-rich halo nucleus ^{8}He because of the very different asymptotic behavior of this weakly bound system. The obvious remedy is to use the s.p. basis that is optimal for a given nucleus, that is, the HF basis. However, since the Berggren ensemble used in the GSM is required to possess spherical symmetry, HF calculations must be constrained to spherical shapes. Moreover, since in some cases one is interested in unbound nuclei lying beyond the drip line (particle resonances), the HF procedure has to be extended to unbound states. In the following, the HF-based procedure that meets the above criteria is referred to as the Gamow-Hartree-Fock (GHF) method.

Since, strictly speaking, the spherical HF potential cannot be defined for open-shell nuclei, one has to resort to approximations. In this work, we tried two different ways of averaging the HF potential. The first ansatz is the usual uniform-filling approximation in which HF occupations are averaged over individual spherical shells. In the second ansatz, the deformed HF potential corresponding to nonzero angular momentum projection is averaged over all the magnetic quantum numbers. Both methods reduce to the true HF potential in the case of closed-shell nuclei.

A. Average spherical HF potential

In the uniform-filling approximation no individual HF orbitals are blocked. The matrix elements of the HF potential U_{uf} between two spherical states α and β carrying quantum numbers (j, l) are

$$\langle\alpha|U_{\text{uf}}|\beta\rangle = \langle\alpha|\hat{h}|\beta\rangle$$
$$+ \frac{1}{2j+1}\sum_{m,\lambda,m_\lambda}\frac{N(\lambda)}{2j_\lambda+1}\langle\alpha m\lambda m_\lambda|\hat{V}|\beta m\lambda m_\lambda\rangle \tag{34}$$

where $\hat{h}$ is the s.p. Hamiltonian (given by a WS +Coulomb potential), λ is an occupied shell with angular quantum numbers (j_λ, l_λ), $N(\lambda)$ is the number of nucleons occupying this shell, and $\hat{V}$ is the residual shell-model interaction.

To define the M potential, one occupies (blocks) the s.p. states in the valence shell that have the largest angular momentum projections on the third axis. The resulting Slater determinant corresponds to the angular momentum $J=M$. For closed-shell nuclei ($M=0$) and for nuclei with one particle (or hole) outside a closed subshell ($M=j$), this Slater determinant can be associated with the ground state of the s.p. Hamiltonian. However, in other cases it corresponds to an excited state with $J>0$. The spherical M potential U_M is defined by averaging the resulting HF potential over magnetic quantum numbers m:

$$\langle\alpha|U_M|\beta\rangle = \langle\alpha|\hat{h}|\beta\rangle + \frac{1}{N_{l,j}}\sum_{m=j+1-N_{l,j}}^{j}\sum_\lambda\langle\alpha m\lambda m_\lambda|\hat{V}|\beta m\lambda m_\lambda\rangle \tag{35}$$

where $N_{l,j}$ is the number of nucleons occupying the valence shell with quantum numbers l, j.

The M potential is expected to work better for nuclei with one particle (or hole) outside the closed subshell. However, one can expect this potential to be not as good as U_{uf} when the Slater determinant with $J=M$ represents an excited state.

B. Unbound HF states

While the HF procedure is well defined for the bound states, it has to be modified for the unbound s.p. states (resonant or scattering), even in the case of closed-shell nuclei. First, the effective nuclear two-body interaction has to be quickly vanishing beyond certain radius. Indeed, if it does not, the resulting HF potential diverges when $r\to+\infty$, thus providing incorrect s.p. asymptotics. Moreover, as resonant states are complex, the true self-consistent HF potential is complex. This is to be avoided, as the Berggren completeness relation assumes a real potential. However, since we are interested in the optimal basis-generating potential and not in the full-fledged complex-energy HF problem [25], we simply take the real part of the (generally complex) HF potential.

C. Treatment of the exchange part

As the residual interaction used in our shell-model calculations is finite range, its exchange part gives rise to a non-local potential. The HF equations solved in the coordinate space can be written as integro-differential equations. The standard method to treat such a HF problem is by means of the equivalent local potential [26]:

$$V_{\text{eq}}(r) = v_l(r) + \frac{\displaystyle\int_0^{+\infty}v_{nl}(r,r')u(r')dr'}{u(r)}, \tag{36}$$

where we use the notation of Eq. (27). The resulting HF equations are local but potentials become state dependent. The main difficulty is the appearance of singularities in $V_{\text{eq}}(r)$ due to the zeros of the s.p. wave function. This problem is practically solved by replacing $u(r)$ with a small number (e.g., 10^{-3}) in the denominator of Eq. (36) when $u(r)$ approaches zero, and by using splines to define the HF potential. The numerical accuracy is checked by calculating overlaps between different wave functions having the same (j, l) values. The overlaps are typically 10^{-5}, which is small enough to consider wave functions orthogonal.

Let us note in passing that the demonstration of Sec. II B is valid when the nonlocal part of the potential is localized, as it is the case for the nuclear interaction. However, if one wants to explicitly consider the Coulomb HF potential between valence protons, one has to resort to approximations in order to avoid its infinite-range nonlocal part. One possibility is to use the so-called Slater approximation, which has been shown to work fairly well [27]. Another method, the so-called generalized local approximation, has been proposed in Ref. [28], where the Coulomb exchange term has been parametrized in terms of a coordinate-dependent effective mass. In any case, the effect of the approximate treatment of the Coulomb exchange term on the GHF basis is very small as compared to other uncertainties related to the construction of the GHF Hamiltonian.

D. Choice of the average potential

In order to compare the quality of two GHF potentials, we inspect the binding energy (i.e., the expectation value of the GSM Hamiltonian) for several Li and He isotopes in the truncated GSM space. As discussed in Sec. V below, we took at most two particles in the GHF continuum. Due to this truncation, and as well as the discretization of the contour L_+ and the assumption of the momentum cutoff (the contour does not extend to infinity), the completeness relation of the resulting many-body shell-model basis is violated and, except for some special cases, the results obtained with different average potentials are different.

According to the variational principle, better basis-generating potentials must yield lower binding energies. Table I shows the binding energies of [6,7,9]He and [7-11]Li calculated in the GSM. Since [8]He and [10]He are closed-shell nuclei, both U_{uf} and U_M are identical in these cases. One can see that the uniform-filling approximation for the GHF potential works better for [7]Li, [8]Li, and [10]Li, whereas the s.p. basis of the M potential is a better choice for [7]He. In all the remaining cases, the two potentials give results that are practically equivalent. In the particular case of [6]He and [6]Li (not displayed), there are *at most* two nucleons in the nonresonant continuum. Consequently, the shell-model spaces for [6]He and [6]Li are almost complete, and the results are almost independent of the choice of s.p. basis. Based on our tests, in our GHF calculations we use the uniform-filling approximation

TABLE I. Binding energies of the He and Li isotopes (in MeV) calculated in the GSM using the GHF basis with (i) the uniform-filling approximation potential U_{uf} or (ii) the U_M potential. See Sec. IV A for definitions.

	^{6}He	^{7}He	^{9}He	^{7}Li	^{8}Li	^{9}Li	^{10}Li	^{11}Li
U_{uf}	-1.038	-0.048	-2.357	-14.266	-15.521	-20.288	-18.082	-15.649
U_M	-0.984	-0.475	-2.418	-13.008	-15.094	-20.181	-17.749	-15.634

except for nuclei with one particle (hole) outside closed sub-shells where the M potential provides a slightly more optimal s.p. basis.

V. GAMOW SHELL-MODEL DESCRIPTION OF THE LITHIUM CHAIN

A. Description of the calculation

In our previous studies [3,4], we have used the s.p. basis generated by a WS potential which was adjusted to reproduce the s.p. energies in ^{5}He. This potential ("^{5}He" parameter set [4]) is characterized by the radius $R=2$ fm, the diffuseness $d=0.65$ fm, the strength of the central field $V_0 = 47$ MeV, and the spin-orbit strength $V_{so}=7.5$ MeV. As a residual interaction, we took the surface delta interaction (SDI). However, when it comes to practical applications, SDI has several disadvantages. First, it has zero range, so an energy cutoff has to be introduced; hence the residual interaction depends explicitly on the model space. Moreover, as the SDI interaction cannot practically be used to generate the HF potential (it produces a nonrealistic mean field), one is bound to use the same WS basis for all nuclei of interest, which is far from optimal as the number of valence particles increases. So, we have decided to introduce [6] a finite-range residual interaction, the surface Gaussian interaction (SGI):

$$V_{J,T}^{SGI}(\mathbf{r}_1,\mathbf{r}_2) = V_0(J,T)\exp\left[-\left(\frac{\mathbf{r}_1-\mathbf{r}_2}{\mu}\right)^2\right]\delta(|\mathbf{r}_1|+|\mathbf{r}_2|-2R_0),$$
(37)

which is used together with the WS potential with the "^{5}He" parameter set.

The Hamiltonian employed in our work can thus be written as follows:

$$\hat{H} = \hat{H}^{(1)} + \hat{H}^{(2)}$$
(38)

where $\hat{H}^{(1)}$ is the one-body Hamiltonian described above augmented by a hard sphere Coulomb potential of radius R_0 from the ^{4}He core, and $\hat{H}^{(2)}$ is the two-body interaction among valence particles, which can be written as a sum of SGI and Coulomb terms. It is important to emphasize that the Coulomb interaction between valence protons can be treated as precisely at the shell-model level as the nuclear part. Indeed, the Coulomb two-body matrix elements in the HF basis can be calculated using the exterior complex scaling as decribed in Ref. [4]. Though not used in this paper, as we are considering only one valence proton in the shell model space, this feature of the Gamow shell model allows for a precise treatment of the Coulomb term.

The SGI interaction is a compromise between the SDI and the Gaussian interaction. The parameter R_0 in Eq. (37) is the radius of the WS potential, and $V_0(J,T)$ is the coupling constant which explicitly depends on the total angular momentum J and the total isospin T of the nucleonic pair. A principal advantage of the SGI is that it is finite range, so no energy cutoff is, in principle, needed. Moreover, the surface delta term in Eq. (37) simplifies the calculation of two-body matrix elements, because they can be reduced to one-dimensional radial integrals. (In the case of other finite-range interactions, such as the Gogny force [29], the radial integrals are two dimensional.) Consequently, with SGI, an adjustment of the Hamiltonian parameters becomes feasible.

The Hamiltonian (38) is diagonalized in the Berggren basis generated by means of the GHF procedure of Sec. IV. This allows one to use the optimal spherical GHF potential for each nucleus studied; hence a more efficient truncation in the space of configurations with a different number of particles in the nonresonant continuum.

B. Choice of the valence space

The valence space for protons and neutrons consists of the $0p_{3/2}$ and $0p_{1/2}$ GHF resonant states, calculated for each nucleus, and the $\{ip_{3/2}\}$ and $\{ip_{1/2}\}(i=1,\ldots,n)$, respectively, complex and real continua generated by the same potential. These continua extend from $\mathrm{Re}[k]=0$ to $\mathrm{Re}[k]=8$ fm^{-1}, and they are discretized with 14 points (i.e., $n=14$). The $0p_{1/2}$ state is taken into account only if it is bound or very narrow. For the lightest isotopes considered, it is a very broad resonant state ($\Gamma \sim 5$ MeV), and, on physics grounds, it is more justified to simply take a real $\{ip_{1/2}\}$ contour, so the completeness relation is still satisfied.

Altogether, we have 15 $p_{3/2}$ and 14 or 15 $p_{1/2}$ GHF shells in the GSM calculation. The imaginary parts of the k values of the discretized continua are chosen to minimize the error made in calculating the imaginary parts of the energies of the many-body states. Other continua, such as $s_{1/2}, d_{5/2},\ldots$ are neglected, as they can be chosen to be real and would only induce a renormalization of the two-body interaction. We have checked [3,4] that their influence on the binding energy of light helium isotopes is negligible. On the other hand, the $1s_{1/2}$ antibound neutron s.p. state is important in the heaviest Li isotopes (^{10}Li, ^{11}Li) and plays a significant role in explaining the halo ground-state (g.s.) configuration of ^{11}Li [9,30]. At present, however, solving a GSM problem for ^{11}Li in the full psd GHF space is not possible within a reasonable computing time.

Having defined a discretized GHF basis, we construct the many-body Slater determinants from all s.p. basis states

TABLE II. Squared amplitudes of different configurations in the ground state of ^{7}Li without truncation (second column) and with truncation to at most two particles in the non-resonant continuum (third column). The sum of squared amplitudes of all Slater determinants with n particles (protons [π] or/and neutrons [ν]) in the non-resonant continuum is denoted by $L_+^{(n)}$.

Configuration	No truncation	Truncation
$0p_{3/2}[\pi]0p_{3/2}^2[\nu]$	$0.561 - i2.783 \times 10^{-4}$	$0.612 - i2.285 \times 10^{-4}$
$L_+^{(1)}[\pi]$	$0.096 + i4.732 \times 10^{-5}$	$0.096 + i4.980 \times 10^{-5}$
$L_+^{(1)}[\nu]$	$0.184 + i1.203 \times 10^{-4}$	$0.164 + i1.077 \times 10^{-4}$
$L_+^{(2)}[\nu^2]$	$0.064 + i2.419 \times 10^{-5}$	$0.054 + i1.600 \times 10^{-5}$
$L_+^{(2)}[\pi\nu]$	$0.088 + i7.032 \times 10^{-5}$	$0.075 + i5.508 \times 10^{-5}$
$L_+^{(3)}[\pi\nu^2]$	$0.088 + i1.621 \times 10^{-5}$	0

(resonant and scattering), keeping only those with at most two particles in the nonresonant continuum. Indeed, according to our tests, as the two-body Hamiltonian is diagonalized in its optimal GHF basis, the weight of configurations involving more than two particles in the continuum is usually quite small, and they are neglected in the following. To illustrate this point, let us consider the $J^\pi = 3/2^-$ ground state of ^{7}Li. Since, in this case, there are only three valence particle, the complete calculation is possible. As seen in Table II, the weight of the component with three particles in the nonresonant continuum, $L_+^{(3)}[\pi\nu^2]$, is indeed two orders of magnitude smaller than other configuration weights. The presence of $L_+^{(3)}[\pi\nu^2]$ modifies the weights of other configurations on a very minor way. For the leading configuration $0p_{3/2}[\pi]0p_{3/2}^2[\nu]$, without any particles in the nonresonant continuum, the effect is $\sim 8\%$. As a consequence, the neglect of the $L_+^{(3)}[\pi\nu^2]$ component leaves the overall structure of the state unchanged, and one can safely truncate the shell-model space while slightly renormalizing the two-body residual interaction.

The algorithm that has been adopted by us [4] to isolate many-body resonances is based on the pole approximation, i.e., the diagonalization of the Hamiltonian in a smaller basis consisting of resonant states only. Therefore, in some cases, it is necessary to include in the GSM basis very broad resonant states. Let us consider, for instance, the first $2^+(T=0)$ state in ^{6}Li and the two lowest $5/2^-$ states in ^{7}Li. Without explicitly taking into account the $0p_{1/2}$ broad Gamow state, the $2_1^+(T=0)$ level of ^{6}Li does not appear in the pole approximation; hence it is very difficult to determine. Similarly, in the same pole approximation, there appears only one $5/2^-$ level in ^{7}Li. Consequently, in order to identify those excited states, we included the resonant $0p_{1/2}$ level in the GSM basis. In order to further reduce discretization effects, we doubled the number of discretization points along the corresponding $0p_{1/2}$ contours. To check whether these two Berggren ensembles are equivalent, we performed calculations for the lowest $1^+, 0^+$, and $2^+(T=1)$ levels in ^{6}Li. (The lowest 3^+ state has not been considered in this exercise, as no $p_{1/2}$ state, resonant or scattering, can enter its decomposition for obvious geometrical reasons.) The results are shown in Fig. 5, from which its is clear that the two GSM bases are practically equivalent.

C. The lithium chain

As a pilot example of GSM calculations in the space of proton *and* neutron states, we have chosen to investigate the Li chain. The continuum effects are very important in these nuclei, both in their ground states and in excited states. The nucleus ^{11}Li is also a well-known example of a two-neutron halo. In our p-space(s) calculation, we consider the one-body Coulomb potential of the ^{4}He core, which is given by a uniformly charged sphere having the radius of the WS potential. It turns out that the inclusion of the one-body Coulomb potential modifies the GHF basis in lithium isotopes as compared to the helium isotopes, an effect which is usually neglected in the standard SM calculations.

Recent studies of the binding energy systematics in the sd-shell nuclei using the shell model embedded in the continuum (SMEC) [31,32] have reported a significant reduction of the neutron-proton $T=0$ interaction with respect to the neutron-neutron $T=1$ interaction in the nuclei close to the neutron drip line [5,33]. In the SMEC, this reduction is associated with a decrease in the one-neutron emission threshold when approaching the neutron drip line, i.e., it is a genuine continuum coupling effect. The detailed studies in fluorine isotopes have shown that the reduction of the $T=0$ neutron-proton interaction *cannot* be corrected by any adjustment of the monopole components of the effective Hamiltonian. To account for this effect in the standard SM, one would need to introduce a particle-number dependence of the $T=0$ monopole terms. Interestingly, it has recently been sug-
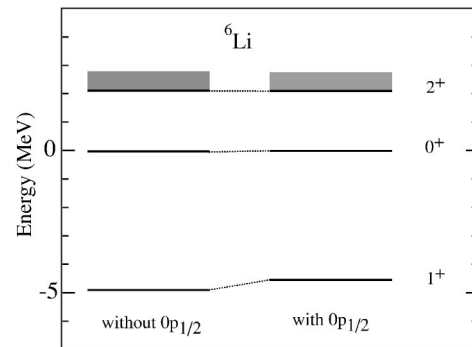

FIG. 5. The lowest $1^+, 0^+$, and $2^+(T=1)$ levels in ^{6}Li calculated with and without the $0p_{1/2}$ s.p. resonant state in the GSM basis.
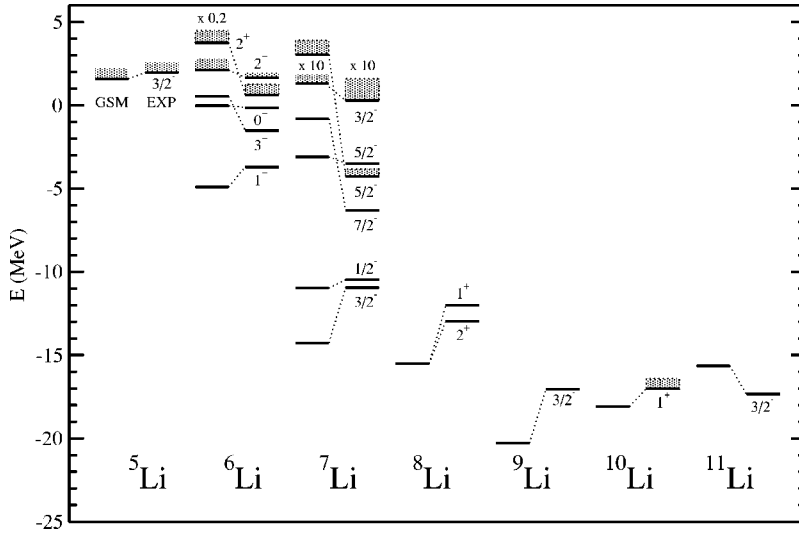
FIG. 6. Experimental (EXP) and predicted (GSM) binding energies and spectra of lithium isotopes obtained with the SGI Hamiltonian. The resonance widths are indicated by shading. The energies are given with respect to the core of ^{4}He. Experimental data are taken from [35–37].

gested [34] that a linear reduction of $T=0$ two-body monopole terms is expected if one incorporates three-body interactions into the two-body framework of a standard SM.

Our GSM studies of lithium isotopes indicate that the reduction of $T=0$ neutron-proton interaction with increasing neutron number is essential. For example, if one uses the $V_0(J,T=0)$ strength adjusted to ^{6}Li to calculate ^{7}Li, the g.s. of ^{7}Li becomes overbound by 13 MeV, and the situation becomes even worse for heavier Li isotopes. To reduce this disastrous tendency, in the first approximation, we have used a linear dependence of $T=0$ couplings on the number of valence neutrons N_n:

$$V_0(J=1,T=0) = \alpha_{10}[1 - \beta_{10}(N_n-1)], \qquad (39)$$

$$V_0(J=3,T=0) = \alpha_{30}[1 - \beta_{30}(N_n-1)], \qquad (40)$$

with $\alpha_{10}=-600$ MeV fm^3, $\beta_{10}=-50$ MeV fm^3, $\alpha_{30}=-625$ MeV fm^3, and $\beta_{30}=-100$ MeV fm^3. This linear dependence is probably oversimplified, as shown in Refs. [5,33] where the proton-neutron $T=0$ interaction first decreases fast with increasing neutron number and then saturates for weakly bound systems near the neutron drip line. For the $T=1$ interaction, we have taken parameters $V_0(J=0,T=1)$ and $V_0(J=2,T=1)$ determined for the He ground states [6], as they provide reasonable results in the He chain.

The results of our GSM calculations for the neutron-rich Li isotopes are shown in Fig. 6. One obtains a reasonable description of the g.s. energies of lithium isotopes relative to the g.s. energy of ^{4}He, but excited states are reproduced roughly. Clearly, the particle-number dependence of the matrix elements has to be further investigated in order to achieve the detailed description of the data. The absence of

an antibound $s_{1/2}$ state in the Berggren basis is also likely responsible for large deviations with the data seen for ^{10}Li and ^{11}Li.

In a number of cases, excited GSM states are calculated to lie above several decay thresholds, i.e., they are predicted to be unstable to single-nucleon, deutron, proton+neutron emission, and/or α decay. The total decay width of a nucleus in a given GSM eigenstate is given by an imaginary part of its complex eigenenergy. Different open decay channels contribute incoherently to the total decay width and their respective partial width cannot be separated easily [2]. In practical applications, however, one may calculate the spectroscopic factors for the separation of nucleon(s) or nucleon groups in a given GSM eigenstate, following the well-known procedures of the standard shell model [38,39], i.e., by calculating the probability to find a certain one- or many-particle configuration formed by A-k and k nucleons in a state of the A-nucleon system. We intend to implement this option in the future.

Due to the explicit presence of the Coulomb potential in the GSM, isospin is no longer conserved. In order to assess the isospin-mixing effect, for each shell-model state $|\Psi\rangle$ we define the average isospin quantum number T_{av} in the following way:

$$T_{av} = \frac{-1 + \sqrt{1 + 4\langle\Psi|\hat{T}^2|\Psi\rangle}}{2} \qquad (41)$$

where the isospin raising and lowering operators in $\hat{T}^2$ act on single-proton and single-neutron states with explicitly *different* asymptotic behavior. As seen in Table III, the values of T_{av} indicate very small isospin-mixing effects. The imaginary part for 2^+ of ^{6}Li and $3/2^-$ of ^{7}Li comes from the fact these states are unbound. This result demonstrates that de-

TABLE III. Average isospin (41) calculated in GSM for various states in ^{6,7}Li.

J^π	1^+	2_1^+	2_2^+	$3/2^-$ (g.s.)	$1/2^-$	$5/2^-$	$7/2^-$	$3/2^-$
T_{av}	0.01	$0.023+i0.020$	$1+i0.015$	0.509	0.514	0.507	0.505	$1.503+i0.011$

spite the presence of the Coulomb potential and despite a large coupling to the continuum in some cases, the isospin quantum number is still almost nearly conserved. That is, isospin is a very good characteristic of nuclear states, even if they are unbound, such as the second $3/2^-$ state of ^{7}Li (which is a $T=3/2$ isobaric analog of the ^{7}He ground state) or the lowest $T=1$, $J^\pi=2^+$ state of ^{6}Li (which can be viewed as a $T=1$ isobaric analog of the first excited state of ^{6}He).

The identification of many-body resonances can be difficult if they lie close in energy and have the same angular momentum and parity. Sometimes isospin can come to the rescue. For instance, the approximate isospin quantum number (41) was used to characterize the two 2^+ states in ^{6}Li and assign their experimental counterparts (see Fig. 6). This method does not work for the two $5/2^-$ levels in ^{7}Li, which have both $T=1/2$. Experimentally, one of these levels is a broad resonance with a width of 880 keV, while the second state has a much smaller width of 89 keV. In our GSM calculations, however, the two lowest $5/2^-$ levels in ^{7}Li differ in their $0p_{1/2}$ content; in the pole approximation one of them contains the $0p_{1/2}$ broad Gamow state while the other does not. Consequently, the latter state can be associated with the $5/2_2^-$ experimental level while the former can be assigned to the broad $5/2_1^-$ resonance.

VI. CONCLUSIONS

The Gamow shell model, which has been introduced only very recently [3,4], has proven to be a reliable tool for the microscopic description of weakly bound and unbound nuclear states. In the He isotopes, the GSM, with either SDI or SGI interactions, was able to describe fairly well binding energy patterns and low-energy spectroscopy, in particular the Borromean features in the chain $^{4-8}$He [4,6]. Using the finite-range SGI interaction made it possible to perform calculations in the GHF basis, thus designing the optimal Berggren basis for each nucleus.

In the Li isotopes, the results crucially depend on the $T=0$ interaction channel. It was found that the $T=0$ force should contain a pronounced density (particle-number) dependence which originates from the coupling to the continuum and leads to an effective renormalization of the neutron-proton coupling. This effect cannot be absorbed by the modification of $T=0$ monopole terms in the standard SM framework. The effective renormalization of $(J=1, T=0)$ and $(J=3, T=0)$ couplings, and, to a lesser extent, other coupling constants found in the present GSM studies have to be further investigated. To better take into account all these effects, calculations with a finite-range, density-dependent interaction inspired by the Gogny force [29] are now in progress. The three main problems related to the realistic GSM calculations are the treatment of the center of mass (essential, especially in the context of halo nuclei), the inclusion of antibound states [9,30,40,41], and the handling of very large shell-model spaces.

For that matter, the successful application of GSM to heavier nuclei is ultimately related to the progress in optimization of the GSM basis, related to the inclusion of the non-resonant continuum configurations. A promising development is the adaptation of the density matrix renormalization group method [42] to the genuinely non-Hermitian SM problem in the complex-k plane using the j scheme [6,43].

In summary, in this paper we report proof-of-principle proton-neutron calculations using the Gamow shell model. Our single-particle proton Hamiltonian contains the Coulomb term that explicitly breaks isospin symmetry. In order to extend GSM calculations to open-proton systems, the Berggren completeness relation has been extended to the case of the Coulomb potential. The completeness relation has also been derived for nonlocal interactions that naturally appear in the GHF method, a Hartree-Fock-inspired procedure to optimize the s.p. basis. According to the GSM, the isospin mixing effects are very weak, even for high-lying unbound states of Li isotopes.

[1] J. Dobaczewski and W. Nazarewicz, Philos. Trans. R. Soc. London, Ser. A **356**, 2007 (1998).

[2] J. Okołowicz, M. Płoszajczak, and I. Rotter, Phys. Rep. **374**, 271 (2003).

[3] N. Michel, W. Nazarewicz, M. Płoszajczak, and K. Bennaceur, Phys. Rev. Lett. **89**, 042502 (2002).

[4] N. Michel, W. Nazarewicz, M. Płoszajczak, and J. Okołowicz, Phys. Rev. C **67**, 054311 (2003).

[5] N. Michel, W. Nazarewicz, J. Okołowicz, M. Płoszajczak, and J. Rotureau, Acta Phys. Pol. B **35**, 1249 (2004).

[6] N. Michel, W. Nazarewicz, M. Płoszajczak, and J. Rotureau, nucl-th/0401036.

[7] R. I. Betan, R. J. Liotta, N. Sandulescu, and T. Vertse, Phys.

Rev. Lett. **89**, 042501 (2002).

[8] R. I. Betan, R. J. Liotta, N. Sandulescu, and T. Vertse, Phys. Rev. C **67**, 014322 (2003).

[9] R. I. Betan, R. J. Liotta, N. Sandulescu, and T. Vertse, Phys. Lett. B **584**, 48 (2004).

[10] T. Berggren, Nucl. Phys. **A109**, 265 (1968).

[11] T. Berggren and P. Lind, Phys. Rev. C **47**, 768 (1993).

[12] P. Lind, Phys. Rev. C **47**, 1903 (1993).

[13] R. Liotta, E. Maglione, N. Sandulescu, and T. Vertse, Phys. Lett. B **367**, 1 (1996).

[14] R. Newton, *Scattering Theory of Waves and Particles* (Springer-Verlag, New York, 1982).

[15] R. Newton, in *Scattering: Scattering and Inverse Scattering in*

Pure and Applied Science, edited by R. Pike and P. Sabatier (Academic Press, San Diego, CA, 2002), p. 686.

[16] P. Morse and H. Feshbach, *Methods of Theoretical Physics* (McGraw-Hill, New York, 1953).

[17] A. Baz, Y. Zel'dovich, and A. Perelomov, *Scattering Reactions and Decay in Nonrelativistic Quantum Mechanics* (Israel Program for Scientific Translations, Jerusalem, 1969).

[18] Y. Zel'dovich, Zh. Eksp. Teor. Fiz. **39**, 776 (1960).

[19] Y. Zel'dovich, Sov. Phys. JETP **12**, 542 (1961).

[20] E. Dolinsky and A. Mukhamedzhanov, Izv. Akad. Nauk SSSR, Ser. Fiz. **42**, 2055 (1977).

[21] B. Gyarmati and T. Vertse, Nucl. Phys. **A160**, 523 (1971).

[22] B. Simon, Phys. Lett. **71A**, 211 (1979).

[23] T. Vertse, R. Liotta, W. Nazarewicz, N. Sandulescu, and A. Kruppa, Phys. Rev. C **57**, 3089 (1998).

[24] P. Lind, R. Liotta, E. Maglione, and T. Vertse, Z. Phys. A **347**, 231 (1994).

[25] A. Kruppa, P.-H. Heenen, H. Flocard, and R. Liotta, Phys. Rev. Lett. **79**, 2217 (1997).

[26] D. Vautherin and M. Vénéroni, Phys. Lett. **25B**, 175 (1967).

[27] J. Skalski, Phys. Rev. C **63**, 024312 (2001).

[28] A. Bulgac, C. Lewenkopf, and V. Mickrjukov, Phys. Rev. B **52**, 16476 (1995).

[29] J. Dechargé and D. Gogny, Phys. Rev. C **21**, 1568 (1980).

[30] I. Thompson and M. Zhukov, Phys. Rev. C **49**, 1904 (1994).

[31] K. Bennaceur, F. Nowacki, J. Okołowicz, and M. Płoszajczak, Nucl. Phys. **A651**, 289 (1999).

[32] K. Bennaceur, F. Nowacki, J. Okołowicz, and M. Płoszajczak, Nucl. Phys. **A671**, 203 (2000).

[33] Y. Luo, J. Okołowicz, M. Płoszajczak, and N. Michel, nucl-th/0211068.

[34] A. Zuker, Phys. Rev. Lett. **90**, 042502 (2003).

[35] H. Bohlen, W. von Oertzen, T. Stolla, R. Kalpakchieva, B. Gebauer, M. Wilpert, T. Wilpert, A. Ostrowski, S. Grimes, and T. Massey, Nucl. Phys. **A616**, 254c (1997).

[36] Evaluated Nuclear Structure Data File, URL http://www.nndc.bnl.gov/ensdf/

[37] Nuclear Structure and Decay Data, URL http://nucleardata.nuclear.lu.se/database/masses/

[38] V. V. Balashov, V. G.. Neudatchin, Yu. F. Smirnov, and N. P. Yudin, Zh. Eksp. Teor. Fiz. **37**, 1387 (1959).

[39] K. Wildermuth, Nucl. Phys. **31**, 478 (1962).

[40] T. Vertse, P. Curutchet, R. Liotta, and J. Bang, Acta Phys. Hung. **65**, 305 (1989).

[41] G. Hagen, M. Hjorth-Jensen, and J. Vaagen, J. Phys. A **37**, 8991 (2004).

[42] S. White, Phys. Rev. B **48**, 10345 (1993).

[43] J. Rotureau, N. Michel, W. Nazarewicz, M. Płoszajczak, and J. Dukelsky (in preparation).